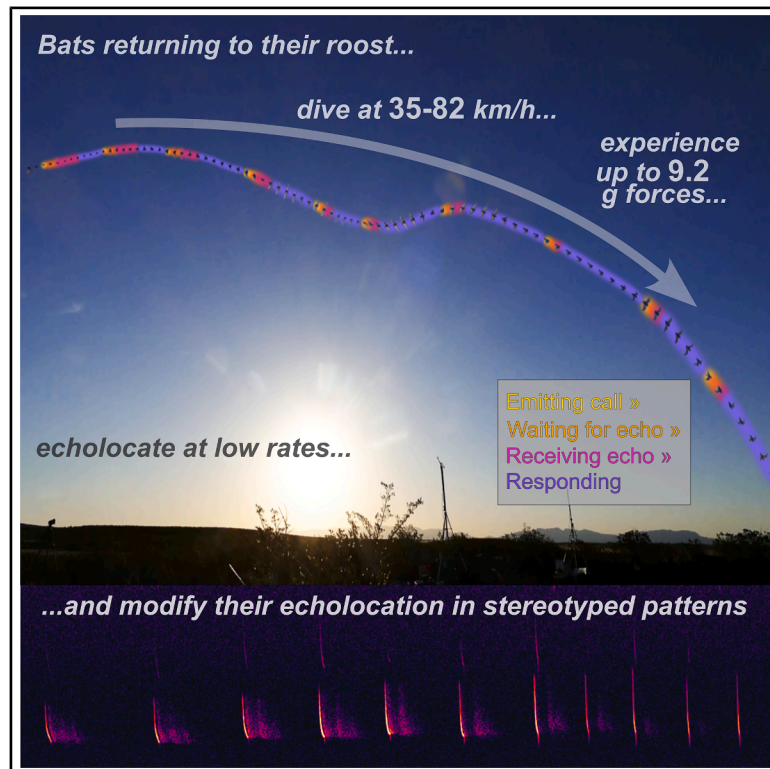


# Stereotyped active sensing in fast-diving echolocating bats

## Graphical abstract



## Authors

Laura N. Kloepper, Amaro Tuninetti, Ian Bentley, ..., Mohammad Rasool Izadi, Robert L. Stevenson, Graham K. Taylor

## Correspondence

[laura.kloepper@unh.edu](mailto:laura.kloepper@unh.edu)

## In brief

Zoology; acoustic signal processing

## Highlights

- Free-tailed bats (*T. brasiliensis*) return to their roosts in steep, fast dives
- Diving bats reach speeds of 82 km/h and experience forces up to 9.2 g
- Bats' flight and echolocation behavior are stereotyped across individuals
- Echolocation timing and frequencies change predictably as bats approach the ground



## Article

# Stereotyped active sensing in fast-diving echolocating bats

Laura N. Kloepper,<sup>1,2,8,\*</sup> Amaro Tuninetti,<sup>1,2</sup> Ian Bentley,<sup>3</sup> Christian D. Harding,<sup>4</sup> Caroline H. Brighton,<sup>6</sup> Mohammad Rasool Izadi,<sup>7</sup> Robert L. Stevenson,<sup>7</sup> and Graham K. Taylor<sup>5</sup>

<sup>1</sup>Department of Biological Sciences, University of New Hampshire, Durham, NH 03824, USA

<sup>2</sup>Center for Acoustics Research and Education, University of New Hampshire, Durham, NH 03824, USA

<sup>3</sup>Department of Physics, Florida Polytechnic University, Lakeland, FL 33810, USA

<sup>4</sup>Division of Pulmonary, Critical Care, Sleep Medicine & Physiology, University of California San Diego Health, San Diego, CA 92103, USA

<sup>5</sup>Department of Biology, Oxford University, Oxford OX12JX, UK

<sup>6</sup>British Trust for Ornithology, Thetford IP242PU, UK

<sup>7</sup>Electrical Engineering, University of Notre Dame, Notre Dame, IN 46556, USA

<sup>8</sup>Lead contact

\*Correspondence: [laura.kloepper@unh.edu](mailto:laura.kloepper@unh.edu)

<https://doi.org/10.1016/j.isci.2025.114099>

## SUMMARY

Mexican free-tailed bats (*Tadarida brasiliensis*) often return to their roosts in darkness or low-light conditions from high altitudes (>3 km) during steep, fast dives. We recorded 26 bats as they performed reentry dives to their canyon roost in New Mexico shortly after dawn and analyzed their sensorimotor behaviors. We tracked bats at altitudes up to 25.6 m above the ground; they dove at maximum speeds of 22.1 m/s (82.1 km/h), experienced forces up to 9.2 g, and traversed distances of up to 6 m (~60 body lengths) between receiving echoes from the ground. Bats adjusted their echolocation in a stereotyped pattern once the ground was within detection range by decreasing signal duration, shortening interpulse intervals, and increasing signal end frequency. Our analyses suggest that bats receive relatively sparse echo information during dives and likely integrate this information with cognitive spatial maps and available visual cues to safely complete their high-speed roost reentry.

## INTRODUCTION

Many animals dynamically adjust their movements to improve the acquisition of sensory information. For visually guided animals, such as insects,<sup>1–3</sup> birds,<sup>4</sup> and most mammals,<sup>5,6</sup> compensatory head or eye movements are used to separate translational from rotational optic flow, which aids in distance estimation and locomotion.<sup>7,8</sup> Aquatic fish and invertebrates move appendages or entire bodies to facilitate the detection of odor cues (see review in Moore et al.<sup>9</sup>) or hydrodynamic flow fields (see review in Fish et al.<sup>10</sup>). Animals that use active sensing, such as electric fish and echolocating bats or odontocetes, modify not only their movements but also their emitted—and hence perceived—signals to improve signal detection in their environment.<sup>11–17</sup>

Bats often navigate and forage in complex, cluttered environments.<sup>18</sup> In order to successfully navigate these environments at high speeds without collisions, echolocating bats combine accurate sensory perception of their environment with motor outputs that are commanded in response to integrated sensory information. While echolocating, auditory feedback drives changes in vocal production, as bats modify their movements and subsequent vocal output on fast time scales in response to changes in sensory information.<sup>19–21</sup>

For example, bats that produce constant-frequency (CF) signals employ Doppler-shift compensation, actively shifting the frequencies of their emitted signals according to flight speed to ensure that returning echoes fall within the narrow frequency range of their most sensitive hearing, thereby maximizing their detection of echoes and prey wing flutter.<sup>22,23</sup> Frequency-modulated (FM) bats do not use the same Doppler-shift compensation as CF bats; instead, they produce signals designed to be tolerant to Doppler effects<sup>24–28</sup> and adjust the characteristics of their signals depending on target distance or environment.<sup>29–31</sup> When tracking targets, bats adjust their flight based on individual echoes,<sup>32–34</sup> typically using information from the most recently returned echo to guide their movement.<sup>35,36</sup> As bats approach objects, they shorten their call duration and interpulse interval (IPI),<sup>30,37</sup> thereby increasing the rate at which they obtain sensory information while simultaneously avoiding pulse-echo overlap<sup>38–41</sup>; at the same time, the bandwidth of their FM pulses widens, facilitating target discrimination and localization.

In certain contexts, bats do not actively modify the parameters of their echolocation based on individual received echoes but rather enter a stereotyped pattern of changing acoustic parameters (APs). For example, when approaching a target, bats predictably reduce the intensity of the emitted signal, irrespective



of target characteristics.<sup>38</sup> When foraging, bats switch from searching to approaching prey in a consistent manner by reducing pulse duration and pulse interval,<sup>37</sup> ending in a terminal buzz of many rapid signals that often continues even after the prey is manually removed or missed.<sup>21,39</sup> When approaching water to drink, bats also use a stereotypical echolocation sequence, reducing the IPI during approach and ending with a buzz and a brief silent period before contact with the water.<sup>40</sup> In both feeding and drinking scenarios, echolocation buzzes are produced at rates faster than the bat's auditory reaction time,<sup>21</sup> providing evidence that bats are not responding to individual echoes.

Most studies describing bat sensorimotor dynamics examine behaviors performed over relatively short flight distances (<10 m) and at speeds less than 4 m/s.<sup>16,33,34,41</sup> However, many bat species fly up to hundreds of kilometers nightly and reach speeds exceeding 30 m/s.<sup>42,43</sup> The cave reentry behavior of free-tailed bats (genus *Tadarida*) is perhaps one of the most dramatic examples of high-speed flight and echolocation behavior. After nightly foraging, individuals return to their roosts in the morning from high altitudes,<sup>42,44</sup> at steep angles and at speeds consistently above 14 m/s, even reaching 44 m/s,<sup>42,43,45</sup> as they locate their cave roost opening. During this high-speed flight, which may have evolved as an antipredator strategy, the wings are held tucked and open only intermittently to control speed and direction.<sup>46</sup> Based on their reported flight speeds<sup>42,45</sup> and typical signal characteristics during reentry,<sup>47</sup> individuals may experience echoes Doppler-shifted by up to 5.7 kHz, which could result in substantial ranging errors.<sup>27</sup> Furthermore, at these high speeds, if bats were producing calls with IPIs consistent with foraging search calls (250 ms<sup>48</sup>), they could travel up to 110 body lengths (~11 m) between receiving consecutive auditory perceptual updates of their environment, leaving only a few hundred milliseconds to react to echoes returning from the fast-approaching ground (due to the relatively short detection range of their echolocation,<sup>49,50</sup> <~50 m; see [supplemental information](#)).

Given the extreme speeds observed during these high-speed entrance dives to their roost, we aimed to evaluate the sensorimotor strategies of wild Mexican free-tailed bats (*T. brasiliensis*) during this behavior. Using synchronized camera arrays and ultrasonic recordings, we reconstructed the 3D path of bats in flight and their biosonar behavior during the dives. From these data, we measured how bats adapt their echolocation behavior depending on height and speed and whether changes in flight trajectory or kinematics coincided with the reception of echoes. Our results demonstrate that, when returning to their roost at fast flight speeds, bats use a consistent, stereotyped echolocation and flight pattern to control their descent and avoid high-speed collisions with the ground. Additionally, bats travel large distances between receiving echo updates and do not change their flight behavior in response to individual echoes. This combination of stereotyped behavior and sparse auditory information suggests that bats do not rely solely on echolocation for their high-speed reentry dives but rather on a combination of integrated auditory, visual, and proprioceptive sensory cues, along with a learned cognitive map of the environment.

## RESULTS

### Flight trajectories

We reconstructed the 3D flight trajectories of 26 individual bats whose reentry was captured on video and used these reconstructed trajectories to calculate kinematic parameters of each bat's flight (Table 1). All bats approached the cave and entered the recorded space from a similar northerly direction, as indicated by the initial tracking angle ( $\overline{\theta_{initial}} = 2.75 \pm 0.84^\circ$ , Figure 1A inset). Bats also consistently left the recorded space at a similar angle ( $\overline{\theta_{final}} = 3.38 \pm 0.45^\circ$ ), dipping below the horizon and out of the camera fields of view as they entered the canyon leading to the cave entrance. Overall, the trajectories of the bats were relatively straight within the recorded area (Figure 1B), as reflected in the high straightness index and low curvature measurements for the majority of bats' trajectories (Table 1).

The height above the ground at which the bats were initially tracked ranged from 9.52 to 25.59 m ( $\bar{h} = 13.69$  m), and the maximum speeds reached by bats during tracking ranged from 11.14 to 22.88 m/s ( $\overline{s_{max}} = 18.12$  m/s), with average speeds between 10.65 and 19.58 m/s ( $\overline{s_{ave}} = 16.45$  m/s). Across bats, speed decreased as they approached the cave entrance (Figure 1C). The high flight speeds, combined with the slight curvature of flight trajectories, resulted in bats experiencing g-forces ranging between 2.56 and 9.21 g ( $\bar{g} = 6.10$  g).

### Echolocation dynamics

Across all bats, we recorded a total of 186 echolocation calls during the period in which they were tracked via video. The emitted calls (corrected for atmospheric absorption and Doppler shift, STAR Methods) were FM downsweeps (Figure 1D), starting at an average of 41.8 ( $\pm 4.7$ ) kHz and ending at 25.9 ( $\pm 1.8$ ) kHz. IPI and call duration averaged 160.8 ( $\pm 51.1$ ) and 8.99 ( $\pm 2.2$ ) ms, respectively. Based on the bats' speed at the time of pulse emission and the peak frequency of their calls, echoes were Doppler-shifted upward by a mean of 3.0 ( $\pm 0.6$ ) kHz. We checked for collinearity of variables prior to model fitting by calculating the matrix of correlation coefficients for the APs of the calls (Table S1). Start frequency, end frequency, and peak frequency were all strongly positively correlated ( $r > 0.65$ ). Bandwidth was very strongly positively correlated with start frequency ( $r = 0.93$ ) but only weakly positively correlated with end frequency ( $r = 0.34$ ). Call duration was moderately negatively correlated with both end frequency ( $r = -0.58$ ) and peak frequency ( $r = -0.51$ ). All other correlations were weak ( $abs(r) < 0.38$ ). As the bats approached the cave, their speed decreased. Figure 2 shows how the measured APs varied with height and speed as the bats approached the cave entrance. Bats produced calls with durations well below the range of pulse-echo overlap, as call duration decreased with height (Figure 2A;  $r = 0.75$ ,  $p < 0.001$ ). IPI also decreased with decreasing height (Figure 2B;  $r = 0.21$ ,  $p = 0.017$ ) but not as consistently as call duration. The end frequency of the recorded signals increased as the bats decreased in height (Figure 2C;  $r = -0.45$ ,  $p < 0.001$ ). These three signal parameters (duration, IPI, and end frequency) did not vary with speed as consistently as

**Table 1. Summary of kinematic parameters for individual bats and across all individuals**

Bat	Max tracked height	Max speed	Min speed	Ave speed	Max <i>g</i>	Straightness index	Ave curvature	Max curvature	Ave pitch angle
1	11.9	15.7	15.1	15.6	4.9	0.98	0.10	0.21	-46.4
2	9.5	11.1	9.9	10.7	4.1	0.94	0.17	0.39	-21.3
3	12.5	18.5	15.6	17.0	6.9	0.98	0.13	0.34	-54.7
4	12.6	17.5	14.3	15.3	7.8	0.75	0.17	0.36	-33.0
5	16.1	14.9	9.7	11.8	5.6	0.79	0.16	0.48	-31.3
6	14.8	19.8	17.0	18.0	6.8	0.98	0.09	0.28	-53.7
7	14.3	16.2	15.0	15.4	6.2	0.98	0.08	0.24	-27.1
8	9.6	17.2	10.8	12.6	7.7	0.46	0.18	0.46	-9.0
9	11.9	16.8	15.9	16.5	4.8	0.99	0.06	0.17	-34.6
10	16.2	20.2	15.3	18.4	8.4	0.88	0.16	0.33	-58.4
11	15.8	20.8	16.2	17.7	5.4	0.98	0.08	0.23	-40.5
12	21.2	19.6	17.2	18.4	8.3	0.90	0.10	0.26	-30.5
13	19.1	17.2	16.0	16.5	2.9	0.98	0.07	0.21	-35.7
14	10.0	17.7	17.4	17.6	4.7	0.99	0.09	0.20	-26.4
15	16.2	17.2	16.1	16.6	3.4	0.98	0.07	0.13	-46.5
16	13.0	18.2	14.1	16.1	7.8	0.97	0.15	0.40	-33.8
17	17.9	19.9	16.3	17.8	7.1	0.98	0.07	0.25	-40.1
18	15.0	18.1	17.1	17.4	5.3	0.99	0.09	0.18	-55.1
19	10.8	15.8	13.2	15.0	8.9	0.61	0.25	0.47	-33.5
20	17.8	19.0	16.6	18.0	6.1	0.99	0.08	0.25	-51.7
21	13.9	18.4	17.0	17.6	6.6	0.96	0.09	0.21	-41.1
22	17.5	20.5	10.5	13.9	9.2	0.43	0.18	0.47	-11.5
23	12.4	18.1	17.4	17.8	2.6	1.00	0.04	0.08	-20.2
24	25.6	22.8	16.7	19.6	5.6	0.96	0.09	0.33	-42.9
25	16.1	18.5	17.2	17.8	4.7	0.99	0.06	0.12	-43.6
26	23.4	22.4	15.9	18.8	7.2	0.96	0.11	0.55	-34.3
Mean	<b>15.2</b>	<b>18.1</b>	<b>15.1</b>	<b>16.5</b>	<b>6.1</b>	<b>0.90</b>	<b>0.11</b>	<b>0.29</b>	<b>-36.8</b>

Height is reported in m, speed in m/s, and pitch angle in degrees relative to the horizon. See STAR Methods for a description of straightness index and curvature. Bold values indicate the mean values for each column.

they did with height (Figures 2D–2F;  $\text{abs}(r)$  values of 0.11–0.31). Bandwidth and peak frequency were also significantly correlated with height, but not with speed (Figure S2).

We built a series of autoregressive generalized linear models (GLMs) to describe the relationship between the APs of the bats' calls and their height and speed as they approached the cave entrance. The results below focus on the models for the three most behaviorally relevant APs in this context: duration, IPI, and end frequency. Call duration is a highly flexible echolocation parameter. FM bats, such as *T. brasiliensis*, generally increase the duration of their calls when flying in open space to increase echolocation range,<sup>51</sup> decrease call durations as they approach an object or surface to avoid temporal overlap between received echoes and emitted calls.<sup>13,52</sup> Similarly, IPI is an extremely flexible echolocation parameter that bats adjust in response to different environments or behavioral contexts, such as foraging and navigating through clutter.<sup>13,53,54</sup> IPI trends are particularly important when approaching surfaces at high speeds, as an overly long IPI could cause a bat to collide with the surface before it has sufficient time to receive an informative echo and respond. End frequency is the most perceptually

important frequency parameter for FM bats,<sup>55</sup> and it shows the strongest relationship with the bats' behavior in our data. The start frequencies at the top of an FM bat's echolocation sweep are more susceptible to atmospheric absorption and travel significantly shorter distances than the lower frequencies of the sweep, which are also emitted in a broader beam than the higher frequencies.<sup>56,57</sup> Accordingly, given the physical limitations of higher frequencies, FM bats appear to rely on the end frequencies of echoes for echo detection and distance perception, while higher echo frequencies are integrated as additional information to perceive more detail.<sup>55,58–60</sup> Additionally, the acoustic recording of the call's upper "start" frequency is heavily influenced by the distance from the bat, the directionality of the bat's beam, and the properties of the microphone used.

Each GLM models an AP as it changes over multiple echolocation calls  $k$  ( $AP_k$ ). For each AP within each model, we considered the first autoregressive acoustic term  $AP_{k-1}$  (i.e., the parameter's value at the *previous* call), the lagged height ( $height_{lag} = height_{k-1}$ ), the change in height between calls ( $\Delta height = height_k - height_{k-1}$ ), the lagged speed ( $speed_{lag} = speed_{k-1}$ ), and the change in speed

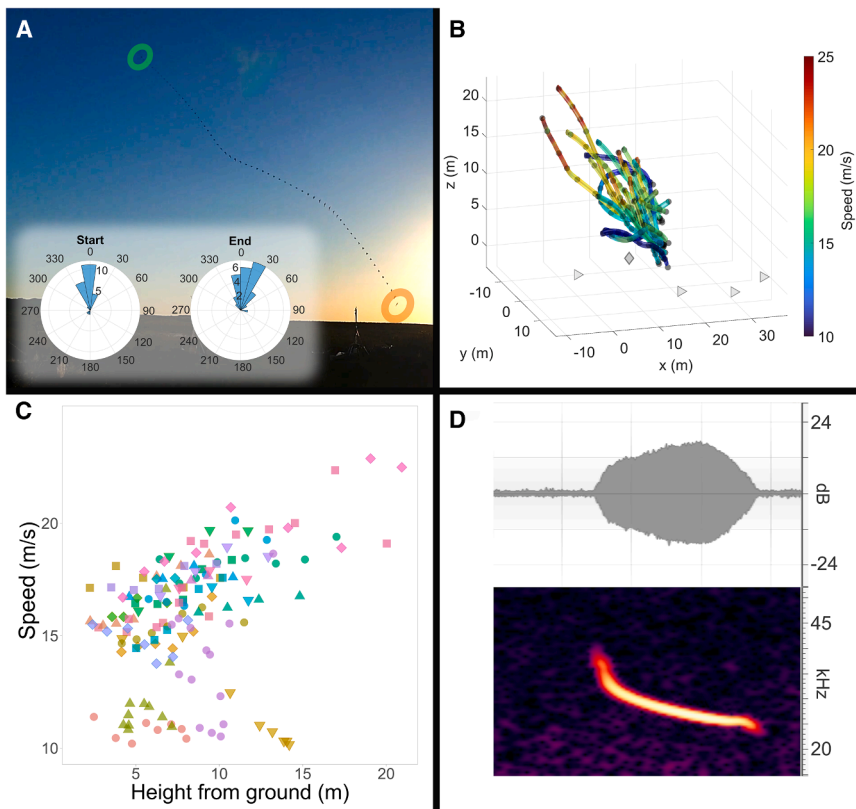


**Figure 1. Summary of bat flight behavior during reentry**

(A) Compilation of cropped video frames from camera 4 showing one bat's flight trajectory. The bat's position in the first frame is circled in green, and its position in the last frame is circled in orange. Inset: polar histograms of the flight directions in which bats are traveling at the start and end of flight tracking.

(B) Reconstructed 3D flight paths of all tracked bats, showing speed (color scale) and positions of echolocation call emissions (gray dots). Triangles indicate video camera positions, and the diamond indicates the position of the ultrasonic microphone.

(C) Flight speed was highly correlated with bat height (individual bats represented by different color-shape combinations).

(D) Waveform and spectrogram showing an exemplar of a recorded echolocation call. Echolocation calls are frequency-modulated (FM) signals beginning around 41 kHz and sweeping downward to approximately 26 kHz.

between calls ( $\Delta speed = speed_k - speed_{k-1}$ ). We included the autoregressive term  $AP_{k-1}$  to control for the nonindependence of consecutive calls, thereby capturing any stereotyped changes in the APs. We included the bat's lagged height and speed (the speed and height of the bat at its previous pulse emission) to model the effects of sensory information received in the previous pulse's echo, thereby capturing the effects of reactive feedforward control. Finally, we included the bat's instantaneous height and speed in the model to capture any predictive feedforward component of the behavior. We compared AICc values to determine the models that best described the collected data; see supplemental information for these comparisons (Table S2), for confidence intervals for each model described below (Table S3), and for model results of other frequency parameters (Table S3).

For call duration (measured in ms), the best model is:

$$duration_k = 1.06 + 0.71(duration_{k-1}) + 0.19(height_{lag}) + 0.46(\Delta height), \quad (\text{Equation 1})$$

which provides evidence that bats control the duration of each call such that (1) it depends in a stereotyped way on the duration of the previous call, becoming approximately 30% shorter with every pulse; (2) it takes into account the most recent sensory information available on the bat's height, becoming shorter the lower the bat's observed height above the ground

the change in height between pulses evidently depends on the bat's dive speed and IPI, there was no strong evidence for a direct effect of speed on call duration.

Likewise, for IPIs (the time from the onset of one call to the onset of the next, in ms), the best model is:

$$IPI_k = 77.09 + 0.44(IPI_{k-1}) + 4.18(height_{lag}) + 24.04(\Delta height). \quad (\text{Equation 2})$$

This model has a similar interpretation to the model for call duration (Equation 2). Specifically, bats command their IPI such that (1) it depends in a stereotyped way on the IPI of the preceding call, becoming approximately 56% shorter with each pulse; (2) it takes into account the most recent sensory information available on the bat's height, becoming shorter the lower the bat's observed height above the ground (estimated effect size: 4 ms per meter above ground); and (3) it has a predictive element with respect to the bat's change in height, becoming shorter the faster the bat approaches the ground between calls (estimated effect size: 24 ms per meter of descent). There was no strong evidence for a direct effect of speed on IPI.

The best model for end frequency ("End Freq," measured in kHz) is:

$$End\ Freq_k = 9.26 + 0.66(End\ Freq_{k-1}) - 0.08(height_{lag}) - 0.31(\Delta height). \quad (\text{Equation 3})$$

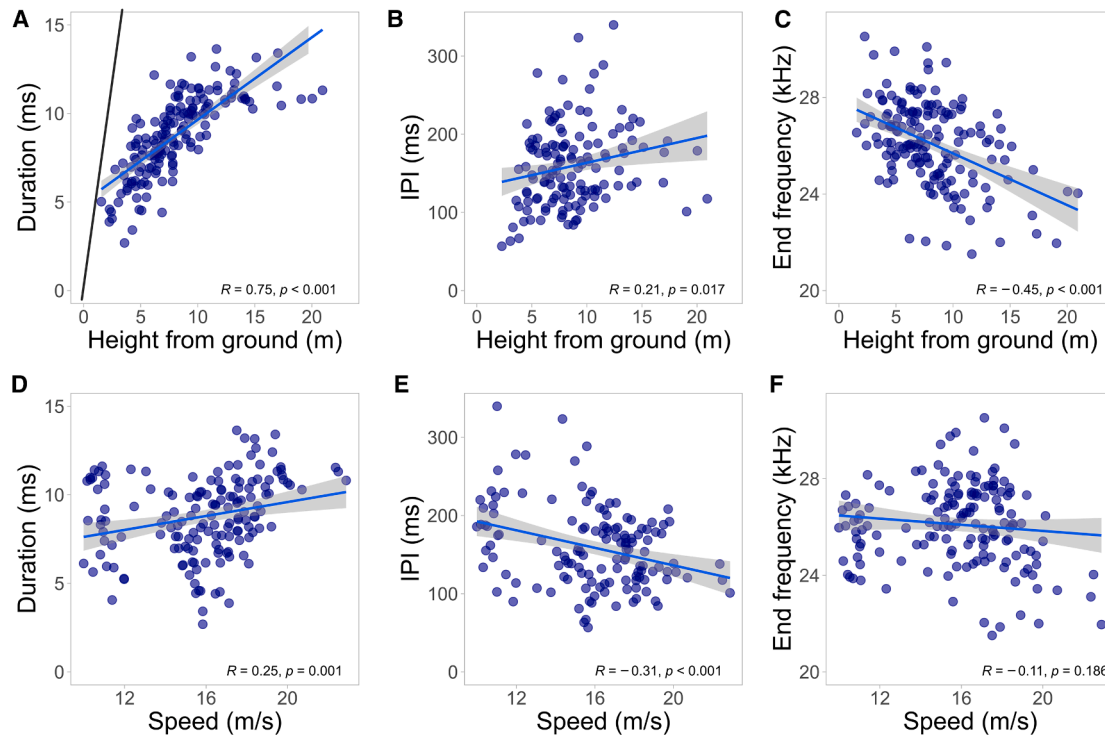


**Figure 2. Changes in acoustic parameters across height and speed of  $N = 26$  bats**

Points indicate individual echolocation calls. Solid lines show the linear regression for each panel's data, with gray shading indicating smoothed 95% confidence intervals. Pearson's  $r$  correlation values and  $p$  values are provided on each plot.

(A) Call durations decrease as bats approach the cave opening, resulting in durations that remain below the limit of call-echo overlap (black line), defined as the time it would take for the reflected echo to return to the bat and potentially interfere with the emitted signal. Note that the longest call durations we observed would have resulted in call-echo overlap had they been emitted at the lowest heights at which bats were calling.

(B) IPI values decrease with decreasing height.

(C) Echolocation end frequencies increase as the bats approach the cave opening.

(D–F) The same acoustic parameters do not vary as strongly with speed. Note that not all data points are independent, as each bat emitted a consecutive series of calls.

This model suggests that bats vary the end frequency of their calls such that (1) it depends in a stereotyped way on the end frequency of the previous call, decreasing by approximately one-third with every pulse; (2) it takes into account the most recent sensory information available on the bat's height, becoming higher in frequency the lower the bat is observed above the ground (estimated effect size: 0.08 kHz per meter above ground); and (3) it has a predictive element with respect to the bat's current height, becoming higher the faster the bat approaches the ground (estimated effect size: 0.31 kHz per meter of descent). There was no strong evidence for a direct effect of speed on end frequency.

### Echo reception and flight kinematics

By combining 3D tracking of bats with the recorded echolocation signals, we were able to calculate the time and location at which each bat emitted each signal, when that signal reflected off the ground (the nearest large reflective surface), and when and where the bat received the ground echo (Figure 3A, see supplemental information). In general, bats did not alter flight kinematics during specific behavioral periods of producing pulses or receiving echoes (Figures 3B and 3C). There was no significant difference in mean curvature or pitch angle between the

acoustic periods of emitting a call, waiting for an echo, receiving the first echo from the ground, and responding to the immediate ground echo while integrating additional echoes before producing the next echolocation call ( $\chi^2(3) = 2.06$ ,  $p = 0.560$ ,  $\chi^2(3) = 0.941$ ,  $p = 0.82$ , respectively). Speed did significantly change as bats transitioned across acoustic phases ( $\chi^2(3) = 14.95$ ,  $p = 0.002$ ), with mean speed significantly decreasing from emitting to waiting ( $Z = -3.625$ ,  $p < 0.001$ ), waiting to receiving ( $Z = -3.823$ ,  $p < 0.001$ ), and receiving to responding ( $Z = -2.786$ ,  $p = 0.005$ ). These results are unsurprising, since bats consistently reduce speed over time as they approach the cave (Figure 1C). From the IPI and flight speed, we calculated an upper limit of 6.1 m for the distance traveled between echolocation pulses, with this distance decreasing as bats approached the cave (Figure 3D). For a subset of recorded bats ( $N = 6$ ), wingtips were sufficiently visible in the video of two or more cameras to allow reconstruction and tracking of the 3D wingtip positions and measurement of wingtip distance to visualize wing movement (see STAR Methods). Across this subset, wing openings coincided with decreases in acceleration, but we did not observe a coupling of sound emission or echo reception with wingbeat phase (Figure S3).

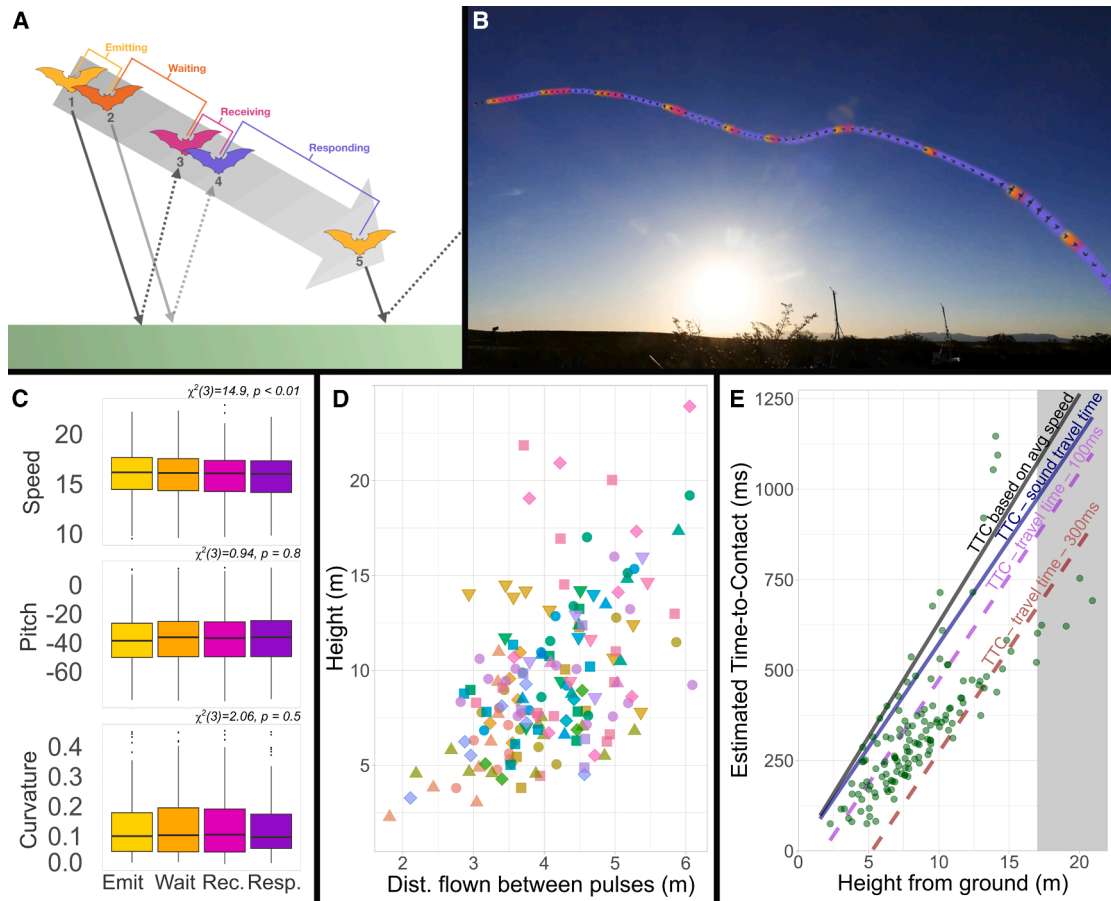


**Figure 3. Sensorimotor dynamics across acoustic phases and height**

(A) Illustration of the acoustic phases, as described in STAR Methods.

(B) Composite images of video frames during reentry for one bat, with acoustic periods indicated by color (emitting, yellow; waiting, orange; receiving, pink; responding, purple).

(C) Boxplots of speed (m/s, top), pitch angle (degrees, middle), and curvature (bottom) across acoustic phase. Boxplots show medians (center horizontal line), first and third quartiles (upper and lower box limit), and whiskers (vertical lines) representing data within 1.5 times the interquartile range; individual points indicate outlier data. Emit, emitting the call, Wait, waiting for the first echo to return, Rec., receiving the first echo from the ground, Resp., responding to the immediate ground echo and integrating additional echoes before producing the next echolocation call. Curvature and pitch angle did not significantly change across acoustic phases ( $\chi^2$  tests,  $p > 0.05$ ), whereas speed demonstrated a consistent reduction across acoustic phases ( $p < 0.01$ ).

(D) Calculated distances traveled by bats between pulse emissions in relation to their height (individual bats represented by different color-shape combinations). Bats traveled a maximum of 6.1 m (~60 body lengths) between pulse emissions, with this distance decreasing as they approached the ground.

(E) Estimated time-to-contact (TTC) with the ground based on bats' heights and speeds. Plotted lines indicate TTC based on average bat speeds and heights (black line); TTC minus the estimated time for a sound to travel to the ground and back (blue line); and TTC minus sound travel time and either 100 ms (pink dashed line) or 300 ms (red dashed line), simulating the time at which a bat would receive an echo when using different IPIs. Green points indicate individual bats' estimated TTC, accounting for sound travel time and their actual IPI. The shaded area represents the theoretical range at which echoes from the ground are first detectable; see supplemental results.<sup>49</sup>

To conceptualize the collision risk bats experience while traveling at such high speeds toward the ground, we calculated the time-to-contact (TTC) with the ground (the rim of the canyon) for each bat based on its height and speed at each echolocation call emission. The calculated TTC also incorporates the air-travel time for the echolocation call to reflect back to the bat and the bat's IPI values at that moment, representing the most delayed timing at which the bats might receive an echo reflected from the ground surface. Figure 3E shows the results of these TTC calculations (green points) along with trendlines

based on bats' average speeds, which show how the bats' TTC is affected by sound travel time (solid lines) and different possible IPI values (dashed lines). This plot shows that, for the majority of the data we recorded, bats had less than 500 ms of time between receiving echoes and reaching the ground surface. The gray dashed bar starting at 17 m indicates the lower range at which we estimate bats begin receiving perceivable echoes from the ground (see supplemental information for details on how we estimated echolocation range<sup>49,50</sup>).

## DISCUSSION

When returning to their roost from altitudes of several kilometers,<sup>44</sup> *T. brasiliensis* fly at high flight speeds and steep angles aimed toward the ground. At the point where we began video tracking, bats had already begun decelerating, yet we documented flight speeds exceeding 22 m/s (82 km/h) and g-forces up to 9 *g*—higher than previously observed in rapidly diving bats.<sup>61</sup> It is likely that, outside of the space we were able to record, these bats fly at even faster speeds and experience higher g-forces. For context, 9 *g* is what trained military pilots experience during their most extreme maneuvers.<sup>62,63</sup> Adult *T. brasiliensis* typically measure ~10 cm in length,<sup>64</sup> and the bats recorded here traveled up to 6.1 m between echolocation calls, meaning they could traverse more than 60 body lengths between receiving auditory updates on the environment ahead of them—roughly equivalent to a human swimmer opening their eyes once every 3.5 laps of an Olympic-length swimming pool. Considering the IPIs and travel time of their echolocation, as well as the short detection range of echolocation, bats were likely often less than 1 s away from colliding with the ground surface at high speed before they began receiving detectable echoes. Within the frequencies emitted by *T. brasiliensis*, the maximum detection range of a large flat surface (such as a meadow or field) ranges from approximately 17–53 m<sup>49</sup> (see [supplemental information](#)), assuming on-axis reflection and maximum source amplitudes; in naturalistic contexts, the maximum detection range is likely even shorter. At the minimum estimated height of 17 m at which bats begin to detect echoes reflected off the ground, and based on the bats' flight speeds and IPIs, most bats would have had less than 700 ms to react to echoes from the ground surface surrounding the canyon entrance (Figure 3E).

Given this feat of sensorimotor control and reaction time, one might expect bats to place great importance on the information contained in each echo, as they use that information to guide their motor behavior over the next 60 body lengths. Contrary to this expectation, we found that fast-diving bats do not significantly alter their flight trajectories in response to individual received echoes (Figure 3C) and instead modify their echolocation in consistent patterns as they descend in height, with APs varying as a result of the previously emitted call, the bat's instantaneous height, and its change in height over time. We propose that the acoustic and locomotive behaviors of bats during cave reentry are “set” at altitudes higher than those at which we were tracking. Bats identify their target (ground and/or cave opening) and begin a stereotyped sensorimotor sequence, which, once initiated, proceeds in a predictable fashion, much like the terminal buzz emitted during foraging or drinking.<sup>21,37,39,40</sup> Some acoustic components of this sensorimotor sequence, such as decreasing call duration to keep it below pulse-echo overlap (Figure 2A), presumably begin once the bat is within detection range of the ground. The ability to identify their target from heights outside echolocation range is likely aided by visual cues, as recordings were during the early dawn hours when ambient light was present.

The statistical models built to describe our collected data suggest that, when bats change their echolocation parameters while diving at fast speeds, they primarily do so in a stereotyped

pattern that is modified according to the bat's height and change in height over time. The observed relationship between echolocation parameters and the bats' height may reflect the fact that echolocation is a relatively short-range sensory system. We recorded bats at a maximum height of 25.6 m, and they were generally already decelerating once they entered the recorded space. Given that bats were approaching their roost (and the recorded space) from higher altitudes and similar directions (Figure 1), we presume that at some point in their descent they transition from not detecting the ground with echolocation to detecting the ground with echolocation. For an echolocating bat, signal duration is one of the primary APs modified as a surface comes into detection range in order to avoid pulse-echo overlap. Correspondingly, we found that bats increasingly shortened their call durations as height decreased, maintaining durations below those that would result in pulse-echo overlap (Figure 2A). In contrast, the end frequencies of emitted signals increased as height decreased, with this relationship being most pronounced below 15 m (Figure 2C). A gradual increase in the end frequency of an FM sweep is a typical and stereotyped response to the appearance and approach of a reflective surface in many bat species,<sup>65,66</sup> indicating that bats are responding to the perceived presence of the upcoming ground surface.

Another common echolocation adaptation that FM bats perform in response to approaching surfaces is a consistent decrease in IPI with decreasing surface distance in order to avoid pulse-echo overlap or pulse-echo ambiguity.<sup>54,58</sup> This is also crucial when approaching a surface at high speed, as longer IPIs reduce the time a bat has to react to an approaching surface (Figure 3E). While IPI was somewhat dependent on the bats' height (see Equation 2 in results), it varied with height much less than signal duration did, with many IPIs remaining above 100 ms (relatively long values) even at heights below 5 m (Figure 2B). However, it is also known that bats significantly and consistently increase their IPI values when flying through well-learned spatial configurations,<sup>41,67–69</sup> even when relying entirely on echolocation for sensory feedback (i.e., when visual information is not available). This likely explains why, in the current context, IPIs remained relatively long after the ground was within detectable range. The bats' spatial memory of the environment and learned flight paths into the cave—which they may navigate nightly for years—allows them to maintain low rates of calling despite their fast flight speeds and rapidly decreasing distance to the ground. Given that much of these bats' navigation back to their roost occurs at heights above which echolocation can assist with terrestrial navigation, it is probable that this spatial understanding of the environment and safe flight paths is built up multi-modally, combining auditory cues with other sensory information such as visual and olfactory cues, and perhaps even social cues or learned behaviors.

Bats' spatial memory capabilities, and the extent to which they underpin navigational abilities, have begun to be better understood in recent years. Advances in tracking technology have allowed for short- and long-term studies of bats' navigational skills, both on daily foraging routes<sup>70–73</sup> and on longer migratory routes.<sup>74</sup> Echolocating bats possess allocentric cognitive maps based on multiscale spatial encoding in the hippocampus,<sup>75,76</sup>

which allow them to perform novel spatial shortcuts without prior experience.<sup>71,72</sup> These cognitive maps are established quickly through teaching and exploration, with juvenile bats establishing home ranges of several tens of square kilometers within 1–2 months of first leaving their natal roost.<sup>70,72</sup> Over shorter distances, bats quickly adopt stereotypical flight paths and flight behaviors even through complex environments,<sup>41,67,69,77</sup> showing that they acquire cognitive representations of spaces at multiple scales, which are then used to help successfully navigate around obstacles. Longer-range migratory routes may not be taught or strictly stereotyped across individuals of a species; individual echolocating bats can take significantly different migratory routes based on environmental and energetic factors.<sup>74</sup>

Beyond the learned cognitive maps that bats acquire over time, it is also important to consider the roles of other sensory modalities during reentry flights. While the visual capabilities of echolocating bats are often underestimated (“blind as a bat”), recent work shows that echolocators, including *T. brasiliensis*, can perceive and respond to visual information—such as ultraviolet light—to a greater extent than previously known,<sup>78–82</sup> which can assist in long-range navigation even under cloud cover.<sup>83,84</sup> Given the altitudes at which these bats forage (well beyond the range at which echolocation can assist with terrestrial navigation) and the ambient light levels during their return to their roost at dawn, it is likely that vision plays a role in navigating back to the roost at dawn, identifying their target, and precisely coordinating their reentry dive. It is possible that we would have observed different sensorimotor behaviors had we also been able to record bats returning to this cave roost before dawn, when ambient light levels were significantly lower. Pre-dawn reentry dives were anecdotally observed by the authors, but our video recording equipment was unable to record at those lower light levels. Prior work exploring changes in echolocation behavior when visual information is present<sup>47</sup> has shown that *T. brasiliensis* modulate echolocation parameters, such as duration and bandwidth, in relation to ambient light when flying near roost entrances, but not when flying in open air. As our current context incorporates both of those environmental layouts (open air transitioning to a roost opening surrounded by acoustic clutter), we might expect to see an even stronger height-dependent modulation of APs in pre-dawn reentry dives than in the results presented here. This previous study<sup>47</sup> was unable to compare echolocation IPI values across ambient light levels, but this is another AP we might expect to differ significantly in pre-dawn conditions, especially considering the large distances we recorded bats traversing between individual echo updates (Figure 3D). In addition to vision, proprioceptive and airflow cues are important for the bats’ ability to control their motor behavior,<sup>85</sup> particularly during high-speed descent and deceleration. Bat wings are covered with fine hairs that are sensitive to both direction and airflow speed,<sup>86–88</sup> providing additional sensory input that must be integrated with information from other modalities to allow for successful navigation at high speeds.

Overall, our results indicate that returning *T. brasiliensis* identify their roost entrance at high altitudes, likely via a combination of visual information and spatial memory, and approach it in stereotyped high-speed dives, during which echolocation param-

eters remain relatively constant until the ground is close enough to be detected. At that point, their echolocation changes in a predictable fashion by decreasing signal duration and increasing end frequency. This roost reentry behavior is a dramatic example of high-speed, high-*g* flight, orientation and navigation, multimodal sensory integration, and sensorimotor control in an active-sensing animal. While we determined that individual bats do not rely heavily on echolocation (especially on the basis of individual echoes) to control their sensorimotor behavior during cave reentry, they nonetheless adapt their echolocation to the current environment in consistent and perceptually relevant ways, such as decreasing call duration to avoid pulse-echo overlap once they are within detectable range of the ground surface. This suggests that, although echolocation occurs at relatively low, stabilized rates in this context, it is adaptable and provides sensory information that would help the bat navigate any short-range obstacles or sudden changes in its environment. What remains less well understood is how bats integrate sensory information from multiple sources to successfully navigate back to their roost, localize it from high altitudes, and accurately dive toward it at speeds exceeding 82 km/h while controlling their descent and avoiding high-speed collisions with the ground. It is also unclear how much of an effect ambient light levels have on the sensorimotor interactions observed here; additional recordings using thermal imagery would be crucial for teasing apart the role of vision in these extreme behaviors. Future work linking acoustic recordings with kinematic parameters—either from longer-range 3D tracking or onboard sensors—is also needed to illuminate the strategies these bats utilize for high-speed flight over long distances.

### Limitations of the study

One central limitation of this study is that data were only collected shortly after sunrise, as our video recording equipment required ambient light to track bats. The video recording setup also limited the distance and altitude at which bats could be tracked, either because distant bats were not captured in the frame of sufficient cameras for localization or because distant bats were too small in the video to be accurately localized. Another limitation is that we only analyzed instances in which a single bat was visible, as we lacked the equipment necessary to correctly assign echolocation calls produced by multiple bats to individual animals.

### RESOURCE AVAILABILITY

#### Lead contact

Requests for further information and resources should be directed to and will be fulfilled by the lead contact, Laura N. Kloepper ([laura.kloepper@unh.edu](mailto:laura.kloepper@unh.edu)).

#### Materials availability

No materials were generated in this study.

#### Data and code availability

- The data for this paper were deposited in an online OSF repository (<https://doi.org/10.17605/OSF.IO/JCW9G>).
- Code for data processing and analysis was deposited in an online OSF repository (<https://doi.org/10.17605/OSF.IO/JCW9G>).

## ACKNOWLEDGMENTS

This project was funded by an Office of Naval Research Young Investigator Award N000141612478 awarded to L.N.K., a National Science Foundation Award (award no. 1916850) awarded to I.B. and L.N.K., and a National Science Foundation Postdoctoral Research Fellowship awarded to A.T. This project also received funding from the European Research Council (ERC) under the European Union's Horizon 2020 research and innovation program (grant agreement no. 682501). We thank Turner Enterprises, Inc., and the Armendaris Ranch for access to and housing at our recording site; Morgan Kinniry, Lucy Giles, Kate McGowan, and Lillias Zusi for fieldwork assistance; and Chloe Crusan for the wingbeat analysis, which was part of her undergraduate thesis.

## AUTHOR CONTRIBUTIONS

L.N.K. and G.K.T. conceptualized the project idea; L.N.K., A.T., C.D.H., and G.K.T. curated the project data; L.N.K., A.T., I.B., C.D.H., M.R.I., and G.K.T. carried out the formal analysis; L.N.K. and G.K.T. acquired funding for the project; L.N.K., C.D.H., C.H.B., R.L.S., and G.K.T. carried out the investigation. L.N.L., C.D.H., M.R.I., and G.K.T. developed the project methodology; L.N.K. administered and supervised the project; L.N.K., I.B., C.D.H., and M.R.I. developed project code and validated the analysis; L.N.K. and G.K.T. supervised the project; L.N.K. and A.T. prepared the original draft of the manuscript and prepared paper visualization; I.B., C.D.H., C.H.B., M.R.I., R.L.S., and G.K.T. reviewed and edited the manuscript.

## DECLARATION OF INTERESTS

The authors declare no competing interests.

## STAR★METHODS

Detailed methods are provided in the online version of this paper and include the following:

- KEY RESOURCES TABLE
- LOCATION AND DATA COLLECTION
- METHOD DETAILS
  - Video analysis
  - Acoustic analysis
- QUANTIFICATION AND STATISTICAL ANALYSIS

## SUPPLEMENTAL INFORMATION

Supplemental information can be found online at <https://doi.org/10.1016/j.isci.2025.114099>.

Received: August 4, 2025

Revised: October 3, 2025

Accepted: November 13, 2025

Published: November 19, 2025

## REFERENCES

1. Kirchner, W.H., and Srinivasan, M.V. (1989). Freely flying honeybees use image motion to estimate object distance. *Naturwissenschaften* *76*, 281–282.
2. Kral, K., and Poteser, M. (1997). Motion parallax as a source of distance information in locusts and mantids. *J. Insect Behav.* *10*, 145–163.
3. van Breugel, F., Morgansen, K., and Dickinson, M.H. (2014). Monocular distance estimation from optic flow during active landing maneuvers. *Bioinspir. Biomim.* *9*, 025002.
4. Bhagavatula, P.S., Claudianos, C., Ibbotson, M.R., and Srinivasan, M.V. (2011). Optic Flow Cues Guide Flight in Birds. *Curr. Biol.* *21*, 1794–1799.
5. Sun, H.-J., Carey, D.P., and Goodale, M.A. (1992). A mammalian model of optic-flow utilization in the control of locomotion. *Exp. Brain Res.* *91*, 171–175.
6. Warren, W.H., Kay, B.A., Zosh, W.D., Duchon, A.P., and Sahuc, S. (2001). Optic flow is used to control human walking. *Nat. Neurosci.* *4*, 213–216.
7. Lee, D.N., Kalmus, H., Longuet-Higgins, H.C., and Sutherland, N.S. (1997). The optic flow field: the foundation of vision. *Philos. Trans. R Soc. Lond B Sci.* *290*, 169–179.
8. Koenderink, J.J. (1986). Optic flow. *Vision Res.* *26*, 161–179.
9. Moore, P., and Crimaldi, J. (2004). Odor landscapes and animal behavior: tracking odor plumes in different physical worlds. *J. Mar. Syst.* *49*, 55–64.
10. Fish, F.E., and Lauder, G.V. (2006). Passive and Active Flow Control by Swimming Fishes and Mammals. *Annu. Rev. Fluid Mech.* *38*, 193–224.
11. Au, W.W.L., and Benoit-Bird, K.J. (2003). Automatic gain control in the echolocation system of dolphins. *Nature* *423*, 861–863.
12. Nachtigall, P.E., and Supin, A.Y. (2008). A false killer whale adjusts its hearing when it echolocates. *J. Exp. Biol.* *211*, 1714–1718.
13. Moss, C.F., and Surlykke, A. (2010). Probing the Natural Scene by Echolocation in Bats. *Front. Neurosci.* *4*, 33.
14. Kloepper, L.N., Nachtigall, P.E., Donahue, M.J., and Breese, M. (2012). Active echolocation beam focusing in the false killer whale, *Pseudorca crassidens*. *J. Exp. Biol.* *215*, 1306–1312.
15. Hofmann, V., Sanguinetti-Scheck, J.I., Künzel, S., Geurten, B., Gómez-Sena, L., and Engelmann, J. (2013). Sensory flow shaped by active sensing: sensorimotor strategies in electric fish. *J. Exp. Biol.* *216*, 2487–2500.
16. Warnecke, M., Lee, W.J., Krishnan, A., and Moss, C.F. (2016). Dynamic echo information guides flight in the big brown bat. *Front. Behav. Neurosci.* *10*, 81.
17. Hofmann, V., Sanguinetti-Scheck, J.I., Gómez-Sena, L., and Engelmann, J. (2017). Sensory Flow as a Basis for a Novel Distance Cue in Freely Behaving Electric Fish. *J. Neurosci.* *37*, 302–312.
18. Schnitzler, H.-U., and Kalko, E.K.V. (2001). Echolocation by Insect-Eating Bats: We define four distinct functional groups of bats and find differences in signal structure that correlate with the typical echolocation tasks faced by each group. *Bioscience* *51*, 557–569.
19. Schuller, G. (1977). Echo delay and overlap with emitted orientation sounds and doppler-shift compensation in the bat. *J. Comp. Physiol.* *114*, 103–114.
20. Übermickel, K., Tschapka, M., and Kalko, E. (2013). Flexible echolocation behavior of trawling bats during approach of continuous or transient prey cues. *Front. Physiol.* *4*, ■■.
21. Geberl, C., Brinkløv, S., Wiegrebe, L., and Surlykke, A. (2015). Fast sensory-motor reactions in echolocating bats to sudden changes during the final buzz and prey intercept. *Proc. Natl. Acad. Sci. USA* *112*, 4122–4127.
22. Schnitzler, H.-U. (1973). Control of doppler shift compensation in the greater horseshoe bat, *Rhinolophus ferrumequinum*. *J. Comp. Physiol.* *82*, 79–92.
23. Schnitzler, H.U., and Denzinger, A. (2011). Auditory fovea and Doppler shift compensation: Adaptations for flutter detection in echolocating bats using CF-FM signals. *J. Comp. Physiol. A Neuroethol. Sens. Neural Behav. Physiol.* *197*, 541–559.
24. Kroszczyński, J.J. (1969). Pulse compression by means of linear-period modulation. *Proc. IEEE* *57*, 1260–1266.
25. Altes, R.A., and Titlebaum, E.L. (1970). Bat Signals as Optimally Doppler Tolerant Waveforms. *J. Acoust. Soc. Am.* *48*, 1014–1020.
26. Boonman, A.M., Parsons, S., and Jones, G. (2003). The influence of flight speed on the ranging performance of bats using frequency modulated echolocation pulses. *J. Acoust. Soc. Am.* *113*, 617–628.

27. Holderied, M.W., Baker, C.J., Vespe, M., and Jones, G. (2008). Understanding signal design during the pursuit of aerial insects by echolocating bats: tools and applications. *Integr. Comp. Biol.* *48*, 74–84.
28. Holderied, M.W., Jones, G., and von Helversen, O. (2006). Flight and echolocation behaviour of whiskered bats commuting along a hedgerow: range-dependent sonar signal design, Doppler tolerance and evidence for 'acoustic focussing'. *J. Exp. Biol.* *209*, 1816–1826.
29. Simmons, J.A., Fenton, M.B., and O'Farrell, M.J. (1979). Echolocation and pursuit of prey by bats. *Science* *203*, 16–21.
30. Surlykke, A., and Moss, C.F. (2000). Echolocation behavior of big brown bats, *Eptesicus fuscus*, in the field and the laboratory. *J. Acoust. Soc. Am.* *108*, 2419–2429.
31. Simmons, J.A., Eastman, K.M., Horowitz, S.S., O'Farrell, M.J., and Lee, D.N. (2001). Versatility of biosonar in the big brown bat, *Eptesicus fuscus*. *Acoust. Res. Lett. Online* *2*, 43–48.
32. Surlykke, A., Ghose, K., and Moss, C.F. (2009). Acoustic scanning of natural scenes by echolocation in the big brown bat, *Eptesicus fuscus*. *J. Exp. Biol.* *212*, 1011–1020.
33. Ghose, K., and Moss, C.F. (2006). Steering by hearing: a bat's acoustic gaze is linked to its flight motor output by a delayed, adaptive linear law. *J. Neuro.* *26*, 1704–1710.
34. Falk, B., Jakobsen, L., Surlykke, A., and Moss, C.F. (2014). Bats coordinate sonar and flight behavior as they forage in open and cluttered environments. *J. Exp. Biol.* *277*, 4356–4364.
35. Webster, F.A., and Brazier, O.G. (1965). "EXPERIMENTAL STUDIES ON TARGET DETECTION, EVALUATION AND INTERCEPTION BY ECHOLOCATING BATS." (SENS SYST LAB TUCSON ARIZ).
36. Masters, W.M., Moffat, A.J., and Simmons, J.A. (1985). Sonar tracking of horizontally moving targets by the big brown bat *Eptesicus fuscus*. *Science* *228*, 1331–1333.
37. Moss, C.F., Bohn, K., Gilkenson, H., and Surlykke, A. (2006). Active Listening for Spatial Orientation in a Complex Auditory Scene. *PLoS Biol.* *4*, e79.
38. Boonman, A., and Jones, G. (2002). Intensity control during target approach in echolocating bats: stereotypical sensori-motor behaviour in Daubenton's bats, *Myotis daubentonii*. *J. Exp. Biol.* *205*, 2865–2874.
39. Kalko, E.K.V., and Schnitzler, H.-U. (1989). The echolocation and hunting behavior of Daubenton's bat, *Myotis daubentonii*. *Behav. Ecol. Sociobiol.* *24*, 225–238.
40. Kloepper, L.N., Simmons, A.M., and Simmons, J.A. (2019). Echolocation while drinking: pulse-timing strategies by high-and low-frequency FM bats. *PLoS One* *14*, e0226114.
41. Tuninetti, A., Ming, C., Hom, K.N., Simmons, J.A., and Simmons, A.M. (2021). Spatiotemporal patterning of acoustic gaze in echolocating bats navigating gaps in clutter. *iScience* *24*, 102353.
42. McCracken, G.F., Safi, K., Kunz, T.H., Dechmann, D.K.N., Swartz, S.M., and Wikelski, M. (2016). Airplane tracking documents the fastest flight speeds recorded for bats. *R. Soc. Open Sci.* *3*, 160398.
43. O'Mara, M.T., Amorim, F., Scacco, M., McCracken, G.F., Safi, K., Mata, V., Tomé, R., Swartz, S., Wikelski, M., Beja, P., et al. (2021). Bats use topography and nocturnal updrafts to fly high and fast. *Curr. Biol.* *31*, 1311–1316.e4.
44. Williams, T.C., Ireland, L.C., and Williams, J.M. (1973). High Altitude Flights of the Free-Tailed Bat, *Tadarida brasiliensis*, Observed with Radar. *J. Mammal.* *54*, 807–821.
45. Marques, J.T., Rainho, A., Carapuço, M., Oliveira, P., and Palmeirim, J.M. (2004). Foraging behaviour and habitat use by the European free-tailed bat *Tadarida teniotis*. *Acta Chiropt.* *6*, 99–110.
46. Davis, R.B., Herreid, C.F., and Short, H.L. (1962). Mexican Free-Tailed Bats in Texas. *Ecol. Monogr.* *32*, 311–346.
47. McGowan, K.A., and Kloepper, L.N. (2020). Different as night and day: wild bats modify echolocation in complex environments when visual cues are present. *Anim. Behav.* *168*, 1–6.
48. Schwartz, C., Tressler, J., Keller, H., Vanzant, M., Ezell, S., and Smotherman, M. (2007). The tiny difference between foraging and communication buzzes uttered by the Mexican free-tailed bat, *Tadarida brasiliensis*. *J. Comp. Physiol.* *193*, 853–863.
49. Stilz, W.-P., and Schnitzler, H.-U. (2012). Estimation of the acoustic range of bat echolocation for extended targets. *J. Acoust. Soc. Am.* *132*, 1765–1775.
50. Stilz, W.-P. (2012). Echolocation range calculator. <http://www.biosonarlab.uni-tuebingen.de/rangecalculator/index.html>.
51. Simmons, J.A., and Stein, R.A. (1980). Acoustic imaging in bat sonar: Echolocation signals and the evolution of echolocation. *J. Comp. Physiol.* *135*, 61–84.
52. Obrist, M.K., and Obrist, M.K. (1995). Flexible bat echolocation: the influence of individual, habitat and conspecifics on sonar signal design. *Behav. Ecol. Sociob.* *36*, 207–219.
53. Neuweiler, G. (2000). *The Biology of Bats* (Oxford University Press, Inc.).
54. Petrites, A.E., Eng, O.S., Mowlds, D.S., Simmons, J.A., and DeLong, C.M. (2009). Interpulse interval modulation by echolocating big brown bats (*Eptesicus fuscus*) in different densities of obstacle clutter. *J. Comp. Physiol. A Neuroethol. Sens. Neural Behav. Physiol.* *195*, 603–617.
55. Bates, M.E., Simmons, J.A., and Zorikov, T.V. (2011). Bats use echo harmonic structure to distinguish their targets from background clutter. *Science* *333*, 627–630.
56. Hartley, D.J., and Suthers, R.A. (1989). The sound emission pattern of the echolocating bat, *Eptesicus fuscus*. *J. Acoust. Soc. Am.* *85*, 1348–1351.
57. Jakobsen, L., Brinkløv, S., and Surlykke, A. (2013). Intensity and directionality of bat echolocation signals. *Front. Physiol.* *4*, 89.
58. Hiryu, S., Bates, M.E., Simmons, J.A., Riquimaroux, H., and Riquimaroux, H. (2010). FM echolocating bats shift frequencies to avoid broadcast-echo ambiguity in clutter. *Proc. Natl. Acad. Sci. USA* *107*, 7048–7053.
59. Bates, M.E., and Simmons, J.A. (2010). Effects of filtering of harmonics from biosonar echoes on delay acuity by big brown bats (*Eptesicus fuscus*). *J. Acoust. Soc. Am.* *128*, 936–946.
60. Tuninetti, A., Simmons, A.M., and Simmons, J.A. (2022). Amplitude discrimination is predictably affected by echo frequency filtering in wide-band echolocating bats. *J. Acoust. Soc. Am.* *151*, 982–991.
61. Voigt, C.C., Bumrungsri, S., and Roeleke, M. (2019). Rapid descent flight by a molossid bat (*Chaerephon plicatus*) returning to its cave. *Mamm. Biol.* *95*, 15–17.
62. Behar, M. (2002). Defying gravity. A small Swiss firm develops an innovative G suit for fighter pilots. *Sci. Am.* *286*, 32–34.
63. Summerfield, D., Raslau, D., Johnson, B., and Steinkraus, L. (2018). Physiologic Challenges to Pilots of Modern High Performance Aircraft" in *Aircraft Technology* (IntechOpen).
64. Schmidly, D., and Bradley, R.D. (2016). "BRAZILIAN FREE-TAILED BAT *Tadarida brasiliensis* (L. Geof. St.-Hilaire 1824)" in the *Mammals of Texas*, 7th edition (University of Texas Press).
65. Ulanovsky, N., Fenton, M.B., Tsoar, A., and Korine, C. (2004). Dynamics of jamming avoidance in echolocating bats. *Proc. Biol. Sci.* *271*, 1467–1475.
66. Cvikel, N., Levin, E., Hurme, E., Borissov, I., Boonman, A., Amichai, E., and Yovel, Y. (2015). On-board recordings reveal no jamming avoidance in wild bats. *Proc. Biol. Sci.* *282*, 20142274.
67. Barchi, J.R., Knowles, J.M., and Simmons, J.A. (2013). Spatial memory and stereotypy of flight paths by big brown bats in cluttered surroundings. *J. Exp. Biol.* *216*, 1053–1063.
68. Yamada, Y., Mibe, Y., Yamamoto, Y., Ito, K., Heim, O., and Hiryu, S. (2020). Modulation of acoustic navigation behaviour by spatial learning in the echolocating bat *Rhinolophus ferrumequinum nippon*. *Sci. Rep.* *10*, 10751.

69. Kong, Z., Fuller, N., Wang, S., Özcimder, K., Gillam, E., Theriault, D., Betke, M., and Baillieul, J. (2016). Perceptual Modalities Guiding Bat Flight in a Native Habitat. *Sci. Rep.* 6, 27252.
70. Goldshtein, A., Harten, L., and Yovel, Y. (2022). Mother bats facilitate pup navigation learning. *Curr. Biol.* 32, 350–360.e4.
71. Toledo, S., Shohami, D., Schiffner, I., Lourie, E., Orchan, Y., Bartan, Y., and Nathan, R. (2020). Cognitive map-based navigation in wild bats revealed by a new high-throughput tracking system. *Science* 369, 188–193.
72. Harten, L., Katz, A., Goldshtein, A., Handel, M., and Yovel, Y. (2020). The ontogeny of a mammalian cognitive map in the real world. *Science* 369, 194–197.
73. Fujioka, E., Nakai, G., Fukui, D., Yoda, K., and Hiryu, S. (2019). Investigation of Large-Scale Navigation Behavior of Echolocating Bats During Natural Foraging, Using GPS and Acoustic-GPS Data-Loggers. In 2019 Proc IEEE Int Conf Pervasive Comput Commun Workshops, pp. 700–702.
74. O'Mara, M.T., Wikelski, M., Kranstauber, B., and Dechmann, D.K.N. (2019). First three-dimensional tracks of bat migration reveal large amounts of individual behavioral flexibility. *Ecology* 100, 1–4.
75. Eliav, T., Maimon, S.R., Aljadef, J., Tsodyks, M., Ginosar, G., Las, L., and Ulanovsky, N. (2021). Multiscale representation of very large environments in the hippocampus of flying bats. *Science* 372, eabg4020.
76. Sarel, A., Palgi, S., Blum, D., Aljadef, J., Las, L., and Ulanovsky, N. (2022). Natural switches in behaviour rapidly modulate hippocampal coding. *Nature* 609, 119–127.
77. Kong, Z., et al. (2013). Optical Flow Sensing and the Inverse Perception Problem for Flying Bats in 52nd Proc IEEE Conf Decis Control, pp. 1608–1615.
78. Marcos Gorresen, P., Cryan, P.M., Dalton, D.C., Wolf, S., and Bonaccorso, F.J. (2015). Ultraviolet Vision May be Widespread in Bats. *Acta Chiropt.* 17, 193–198.
79. Winter, Y., López, J., and Von Helversen, O. (2003). Ultraviolet vision in a bat. *Nature* 425, 612–614.
80. Müller, B., Glösmann, M., Peichl, L., Knop, G.C., Hagemann, C., and Ammermüller, J. (2009). Bat Eyes Have Ultraviolet-Sensitive Cone Photoreceptors. *PLoS One* 4, e6390.
81. Danilovich, S., and Yovel, Y. (2019). Integrating vision and echolocation for navigation and perception in bats. *Sci. Adv.* 5, eaaw6503.
82. Lindecke, O., Elksne, A., Holland, R.A., Pētersons, G., and Voigt, C.C. (2019). Experienced Migratory Bats Integrate the Sun's Position at Dusk for Navigation at Night. *Curr. Biol.* 29, 1369–1373.e3.
83. Greif, S., Borissov, I., Yovel, Y., and Holland, R.A. (2014). A functional role of the sky's polarization pattern for orientation in the greater mouse-eared bat. *Nat. Commun.* 5, 4488.
84. Barta, A., and Horváth, G. (2004). Why is it advantageous for animals to detect celestial polarization in the ultraviolet? Skylight polarization under clouds and canopies is strongest in the UV. *J. Theor. Biol.* 226, 429–437.
85. Horowitz, S.S., Cheney, C.A., and Simmons, J.A. (2004). Interaction of vestibular, echolocation, and visual modalities guiding flight by the big brown bat, *Eptesicus fuscus*. *J. Vestib. Res.* 14, 17–32.
86. Sterbing-D'Angelo, S., Chadha, M., Chiu, C., Falk, B., Xian, W., Barcelo, J., Zook, J.M., and Moss, C.F. (2011). Bat wing sensors support flight control. *Proc. Natl. Acad. Sci. USA* 108, 11291–11296.
87. Sterbing-D'Angelo, S.J., Chadha, M., Marshall, K.L., and Moss, C.F. (2017). Functional role of airflow-sensing hairs on the bat wing. *J. Neurophysiol.* 117, 705–712.
88. Rummel, A.D., Sierra, M.M., Quinn, B.L., and Swartz, S.M. (2023). Hair, there and everywhere: A comparison of bat wing sensory hair distribution. *Anat. Rec.* 306, 2681–2692.
89. Kloepper, L.N., Linnenschmidt, M., Blowers, Z., Branstetter, B., Ralston, J., and Simmons, J.A. (2016). Estimating colony sizes of emerging bats using acoustic recordings. *R. Soc. Open Sci.* 3, 160022.
90. Hedrick, T.L. (2008). Software techniques for two- and three-dimensional kinematic measurements of biological and biomimetic systems. *Bioinspir. Biomim.* 3, 034001.
91. Puckett, J.G., Kelley, D.H., and Ouellette, N.T. (2014). Searching for effective forces in laboratory insect swarms. *Sci. Rep.* 4, 4766.
92. Batschelet, E. (1981). *Circular Statistics in Biology* (Academic Press).
93. Holderied, M.W., Jones, G., and von Helversen, O. (2006). Flight and echolocation behaviour of whiskered bats commuting along a hedgerow: range-dependent sonar signal design, Doppler tolerance and evidence for acoustic focussing. *J. Exp. Biol.* 209, 1816–1826.
94. Boonman, A., and Jones, G. (2002). Intensity control during target approach in echolocating bats: stereotypical sensori-motor behaviour in Daubenton's bats, *Myotis daubentonii*. *J. Exp. Biol.* 205, 2865–2874.
95. Pudlo, A., and Kloepper, L.N. (2019). Echolocation adaptations during high-speed roost re-entry for Brazilian free-tailed bats (*Tadarida brasiliensis*). *J. Acoust. Soc. Am.* 145, EL1–EL6.
96. Hecht, E. (2002). *Optics*, 4th edition (Addison-Wesley).

## STAR★METHODS

### KEY RESOURCES TABLE

REAGENT or RESOURCE	SOURCE	IDENTIFIER
Deposited data		
Data and data processing code	This paper	<a href="https://doi.org/10.17605/OSF.IO/JCW9G">https://doi.org/10.17605/OSF.IO/JCW9G</a>
Software and algorithms		
SPSS v26	IBM	RRID:SCR_002865
MATLAB 2019	Mathworks	RRID:SCR_001622
DLTd v6	Hedrick <sup>90</sup>	<a href="https://doi.org/10.1088/1748-3182/3/3/034001">https://doi.org/10.1088/1748-3182/3/3/034001</a>

### LOCATION AND DATA COLLECTION

We recorded individual *Tadarida brasiliensis* as they returned to their cave roost at the Jornada Cave, New Mexico, USA, which contained approximately 500,000 female bats and their nonvolant young.<sup>89</sup> The cave is composed of a collapsed lava tube located on a flat basaltic lava field in the Chihuahuan desert ecoregion with short (<0.5 m tall) desert scrub. The source volcano is located 2 km at 18° bearing and approximately 100 m elevation relative to the study cave. The cave opening is approximately 10 m in height and 15 m in width and located inside the canyon created by the collapsed lava tube.

### METHOD DETAILS

Video recordings were made at dawn on 23/06/2018 (05:32–07:32) and 24/06/2018 (06:19–07:22) using four Panasonic Lumix DMC-FZ1000 compact digital cameras, each mounted on a tripod with a three-way Manfrotto head and recording 1920 × 1080-pixel video at 50 frames per second. We developed a calibration method in which the poses of cameras could be elucidated using information provided by their mutual visibility; three of the four camera views were used to reconstruct the 3D positions of bats (see [supplemental Materials S1](#)). The specific orientation of the camera system meant that entries of bats arriving from any direction could be captured, however there was a bias for longer flight paths in bats arriving from the North and the East, the direction from which bats had previously been observed to return. The cameras were positioned above the canyon, so we recorded the trajectory of each bat until they dropped below the horizon to enter the cave. Bats were tracked for an average of 114 frames as they moved through the cameras' field of view.

Acoustic recordings were made with an ultrasonic microphone (SMM-U1, Wildlife Acoustics) placed adjacent to one video camera at the edge of the canyon ([Figure 1B](#)) and oriented in the direction from which bats would return, recording at a sample rate of 256 kHz. The microphone was visible in all video cameras for extraction of its 3D position. The microphone and video cameras were manually synchronized every 5 min throughout the recording period, and we verified no frame drift in the camera synchronization across each 5-min interval. By combining the acoustic and video recordings, we reconstructed the 3D locations at which bats emitted echolocation calls and additionally calculated the 3D locations at which they received an echo from the ground (the nearest large reflective surface; see [supplementary materials S2](#) and [Figure S1](#)).

#### Video analysis

From the video footage, we manually identified 26 entry flights simultaneously visible in all four cameras in which only one bat was present and thus could be identified as the source of temporally coinciding echolocation calls. For each flight, the videos from the cameras were individually run through the MATLAB application DLTdv6<sup>90</sup> to determine X and Y coordinates for the center of mass of the bat in each frame, and spline interpolation was used to smooth the 3D flight path coordinates. The 3D position of the recording microphone was also determined by reconstructing the position of the microphone within the camera model using its 2D coordinates in the views of cameras 2–4. Details on the generation of the camera model and reprojected pixel error can be found in [supplementary Materials S1](#).

For each bat, we determined the following instantaneous kinematic parameters during reentry: speed, acceleration, curvature (calculated as the inverse of the radius of curvature in meters<sup>91</sup>), pitch angle relative to the horizon, and g-force. We determined the overall straightness index, defined as the ratio between the length of a straight line connecting the start and ending points of the bat compared to the actual length of the path traveled by the bat.<sup>92</sup> Furthermore, for bats in which wingtips were clearly visible ( $N = 6$ ), we determined the distance between wingtips to examine wing movement during flight.

#### Acoustic analysis

We mapped the acoustic data onto the trajectory data in a two-step process designed to match the start of each received echolocation call to the point on the trajectory closest to the time at which the call was actually emitted. As a first step, we used the

photogrammetric data to determine the bat's distance to the ultrasonic microphone at the time the call was received. We used this distance to give a first-order approximation of the travel time between emitter and receiver, and hence a first estimate of the time at which the call was emitted. As a second step, we used the photogrammetric data to determine the bat's distance to the ultrasonic microphone at our first estimate of the emission time. We then used this distance to give a second-order approximation of the travel time, and hence an improved estimate of the time at which the call was emitted. This method was sufficient to determine to within  $\pm 20$  ms the point on the trajectory closest to the time at which the call was actually emitted, this stated accuracy corresponding to the sampling interval of the video recordings.

## QUANTIFICATION AND STATISTICAL ANALYSIS

Each recorded call was corrected for atmospheric absorption and Doppler shift based on the speed of the bat and distance to the microphone.<sup>93–95</sup> The peak frequency, start frequency ( $-10$  dB relative to peak), end frequency, duration, bandwidth, and interpulse interval (IPI) were also calculated for each echolocation signal. To investigate the separate effect of speed and height on pulse duration, peak frequency, start and end frequency, bandwidth, interpulse interval, and responding time, we built a series of autoregressive generalized linear models (GLMs), with all statistics conducted in SPSS v. 26. We compared GLM performance using AICc values; see Supplementary materials for these comparisons (Table S2), for confidence intervals for each of the models described below (Table S3), and for model results of other frequency parameters (Table S3). We additionally simulated the results of each of our GLMs by using combinations of different starting values for each parameter and simulating how those affect subsequent acoustic parameters over the course of multiple sequential calls (Figures S4–S6).

In addition to extracting call parameters, we also calculated the time delay of received direct echoes as bats approached the cave by combining the acoustic data with the video data. Because the video data yielded a frame resolution of 20 ms, but the call durations were typically between 6 and 12 ms, we first used a linear spline technique in MATLAB to interpolate the locations at all times in between the tracked frames on a 1 ms time step. We then assumed that the majority of the sound reflection would be made off of the ground below, because it is the largest and closest flat object near the bat that it is heading toward. We then used the position in which a call was made, combined with the law of reflection,<sup>96</sup> and speed of the bat to determine the position and time when the bat's flight would intersect any forward-facing echo (see supplementary section S2 for details).

To investigate how behavioral state affected flight kinematics, and thus determine if bats were altering flight path during periods of receiving echo information, we identified, based on the timing of call emission and received echoes, the following acoustic phases: (a) "emitting," defined as the period in which the bat is emitting the call, (b) "waiting," defined as the period between the end of call emission at the start of echo reception; (c) "receiving," defined as the period in which the bat is receiving the echo from the ground; (d) "responding," defined as the period between when the bat has stopped receiving the ground echo but before next call emission. See Figure 3A for an illustration of these periods and supplemental materials for how the ground echo was calculated. We then compared the mean curvature, speed and pitch angle between the acoustic time phases using a Friedman test with post hoc Wilcoxon signed-rank tests and Bonferroni correction, resulting in a significance level set at  $p < 0.017$ . To understand how the changes in acoustic behavior during cave approach impact the sensory risk to a bat, we calculated distance traveled between pulses. The distance traveled between pulses was calculated by multiplying the IPI by the speed at the time of pulse emission.